

# A System for Improving the Diagnostic Quality of Fetal Electrocardiogram

**Abstract.** This article deals with utilisation of adaptive filtration for improvement of the diagnostic quality of fetal electrocardiogram as a modern tool used in prediction of intrapartum fetal hypoxia. In the case of the latest intrapartum monitoring method, the quality of the curve of fetal electrocardiogram has a major influence on the quality of the fetal monitoring. The aspect subjected to the diagnostic analysis is the ST interval of the ECG curve. In today's medical diagnostic technology this advanced method is only applied in internal monitoring systems. The authors of this study concentrate on external monitoring which, contrary to the classic internal monitoring, brings about a number of problems regarding the quality of recordings.

**Streszczenie.** W artykule zaproponowano filtr adaptacyjny w celu poprawy jakości elektrokardiogramu płodu. Dotychczas stosowano taką metodę do wewnętrznych systemów monitorowania. Autorzy rozszerzyli tę metodę także na systemy zewnętrzne. (Metoda poprawy jakości diagnostyki przy wykorzystaniu elektrokardiogramu płodu).

**Keywords:** fetal electrocardiogram, ST segment, external monitoring, adaptive filtration.

**Słowa kluczowe:** elektrokardiogram płodu, filtry adaptacyjne.

## Introduction

If the external monitoring is used for the analysis of the fetal cardiac activity in real conditions, such analysis is impaired by a series of undesired signal components. These include above all superposing of the mother's stronger electrocardiogram, power frequency and various motion artifacts. For this reason the current dynamic medical devices do not facilitate a precise analysis of ST segment by means of external monitoring. Current methods of the intrapartum external monitoring are not able to detect fetal hypoxia. However, standard methods used for the analysis of fetal electrocardiogram appear to be insufficient. The authors present a complex solution in the form of a system for elimination of the undesired signal components which degrade the signal under examination, based on the measurements of real ECG signals [6]. The results of the experiments indicate that the adaptive system using the RLS algorithm may be used with the STAN system [12] which applies the latest methods of the ST interval analysis for the diagnostics of fetal hypoxia during labour. The designed adaptive system has the ambition to clear up any doubts regarding evaluation of the results of the ST analysis using the gentler external monitoring method.

In medicine, biological signals serve the purpose of expressing information about a biological system, i.e. an organism. It is therefore necessary to process the biosignals appropriately in order to gain the required information. In this study, the authors focus on the processing of the ECG signals (Electrocardiography) [14] by means of adaptive filtration. The ECG (Fig.1) represents a basic non-invasive method of functional examination of the electric activity of myocardium [6]. Cardiac activity is characterised by a considerable synchronism and periodicity in comparison with other biosignals, such as CNS (*Central Nervous System*) [11]. An ECG signal (Fig. 1) travels from the myocardium in all directions to the whole body and it is measurable all over the body surface (the amplitude ranging between units and tens of mV).

Fetal electrocardiograph (FECG) is the latest method of intrapartum monitoring [7]. This modern electronic monitoring technique utilising cardioflowgraphy enables continuous monitoring of the reactions of the fetus by means of analysing its cardiac activity. The technique brings about a unique opportunity to identify fetal hypoxia [7] and thus prevent brain damage. Fetal hypoxia and stress are reflected by a change of the T wave on the FECG (Fig. 4). It has been proved that by means of

analysis of the FECG curve a significant reduction in the number of hypoxic neonates has been achieved [8]. Today's medical measuring devices allow for monitoring of the fetal heart frequency performed in both external (abdominal) and internal (direct, intrauterine) ways. In case of using the non-invasive external methods of FECG monitoring, we have to deal with elimination of undesirable signal components (noises).

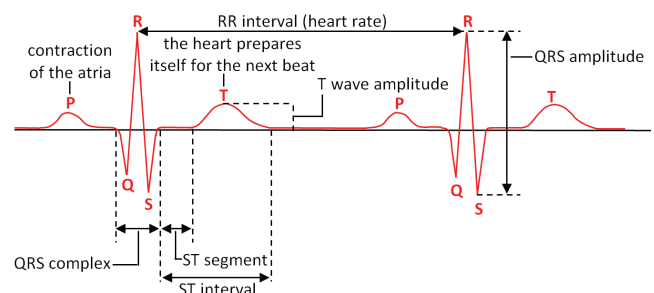


Fig.1. The description of the ECG curve

This study analyses the synthetic filtration techniques [1] based on adaptive filtration which offers solution to the problems related to the FECG analysis. An adaptive system for filtration of the undesirable signal components of the FECG is presented in this paper. In this case it is not possible to use the traditional filtration techniques [3] due to the time variability of the spectrum of both the interfering and the useful signals. Two basic representatives of the adaptive algorithms were selected for the experiments, namely the LMS algorithm based on stochastic gradient adaptation [4] and the RLS algorithm based on optimum recursive adaptation [4].

## Fetal electrocardiograph

In general, there are two methods of FECG extraction. The first, invasive method involves attaching a scalp electrode [21] directly to the head of the fetus (Fig. 2b); however, this method is very uncomfortable [21]. The second method involves extracting the FECG using the electrodes placed on the mother's abdomen (Fig. 2a). This non-invasive progressive method is what the authors of this article focus on exclusively in here. One of the undisputed advantages of the non-invasive method is the fact that the fetus does not receive any energy, which allows for the performance of long-term studies. Application of a

traditional external probe without implementing the modern filtration technology only enables recording of the R-R interval [22], i.e. the time segment between the individual heart beats of the fetus. This technique cannot be used to detect the complete fetal ECG curve.

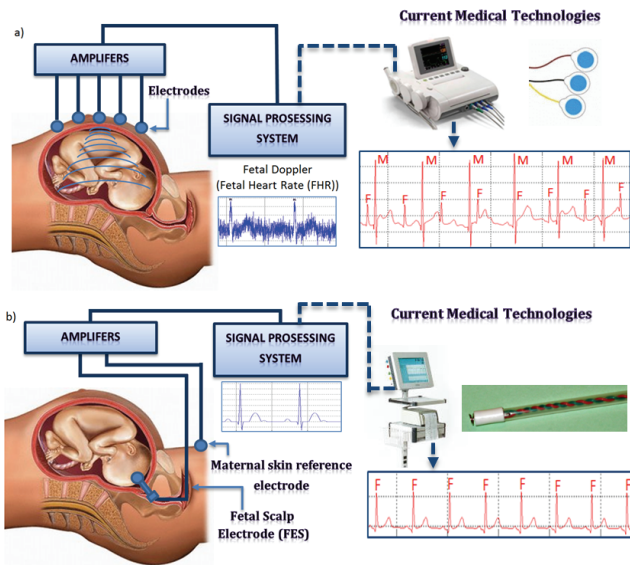


Fig.2. The fetal ECG monitoring a) external b) internal

### Problems related to the abdominal monitoring method

The use of the gentler (non-invasive) external method brings about a number of problems, mainly a great degree of noises interfering with the FECC signal, which consequently becomes unreadable for further evaluation (diagnosis). Above all, the FECC signal gets contaminated to a great extent by the MEEG signal (the mother's ECG), characterised by much higher amplitude (Fig. 3).

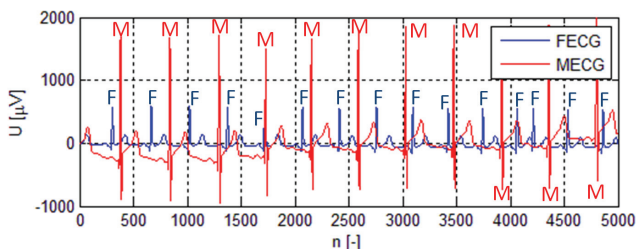


Fig.3. The weaker FECC and the stronger MEEG signals

There are a series of other, non-cardiac sources of interference occurring during the FECC extraction. The narrowband signals: isoelectric line oscillation (electrochemical processes on the electrode-skin interface (from 0.8 Hz), breathing (from 0.5 Hz), slow body motions (from 1.5Hz), power line interference (induction from the mains distribution system (EU 50Hz, USA 60Hz)). The broadband signals: myopotentials and motion aspects (active muscle motions (from 20Hz to several kHz)), rapid changes of the isoelectric line (bad contact of the scanning electrode (15Hz, sporadically 20Hz), impulse disturbance (technical aspects – e.g. other medical devices – hard to eliminate) [7], [8], [9] and [30].

### Analysis of the ST segment

In 1999 a new approach towards the analysis of fetal hypoxia during labour was introduced, the so-called STAN system (the ST segment analysis) on the fetal ECG [22]. During the state of hypoxemia, the  $\beta$ -adrenergic receptors

and anaerobic glycogenolysis are activated [21]. This process results in the release of lactic acid and potassium, leading to a change of the potential of the myocardium cell membrane. From the viewpoint of the ECG curve diagnostics, this process is reflected by an elevation of the ST segment (Fig. 4) [21]. Hypoxemia further stimulates secretion of adrenaline, which results in an increased contraction activity of the myocardium and further induces glycogenolysis [21]. This brings about an elevation of the T-wave on the ECG again. If the hypoxemia develops into a serious form of hypoxia, the ST segment shows a depression. The myocardium is no longer able to react to the oxygen deficiency and cope with deepening hypoxemia. The whole process leads to a reduced myocardium activity and gradually increases the risk of cardiovascular failure. The depression of the ST segment combined with the T-wave elevation or a biphasic shape of the ST segment are indicators predicting myocardial ischemia. For more details refer to [21], [20],[ 24] and [30].

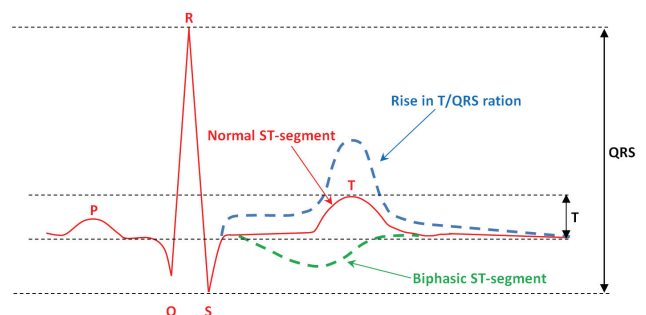


Fig.4. Changes of the fetal ECG during hypoxia: elevation of ST segment – reaction of the myocardium to hypoxia, depression of ST segment – the fetus has run out of its reserves, it is not able to cope with deepening hypoxia

It is clear from the facts stated above that there is a need for a very precise evaluation of the FECC curve (ST segment). At present this issue is being dealt with by a number of academic settings all over the world. A whole series of methods has been developed up to now, characterised by different approaches towards improvement of the informative value of the FECC, such as blind source separation (BSS) [24], [26], wavelet based methods [9], [27], singular value decomposition (SVD) and independent component analysis (ICA) [24], [25], matching pursuits [28], auto-correlation and cross-correlation techniques [29], etc. Generally, none of these approaches have reached satisfactory results in the FECC processing. Certain FECC processing techniques such as SVD or the wavelet based methods have shown good experimental results; however, they are very scarcely used in practice as their application is connected with many problems [30].

The most convenient approach seems to be the method based on the adaptive filtration with regard to real-time processing, computational complexity and simplicity of implementation. In general, an adaptive system with the implemented LMS algorithm was the first system to offer a successful solution to the problem of the FECC curve analysis. The authors of this article concentrated on the latest approach towards the FECC analysis using STAN. Here the adaptive system based on the LMS algorithm reached its limits, mainly due to the low convergence speed and worsened monitoring ability. The experiments performed within this study included simulations using LMS and RLS algorithms. The algorithms of the RLS family appear to be very convenient for the solution of the FECC extraction problem, especially thanks to their high convergence speed. In the past, these algorithms were not

widely used because of a high level of computational difficulty. Nowadays we already have sufficiently powerful (multicore) digital signal processors to be able to process these algorithms in real time.

### Situation in the year 2011

Accurate detection of fetal hypoxia during labour is a great challenge for contemporary obstetrics. The currently used methods of intrapartum fetal monitoring are not sufficiently precise. The use of stethoscope now belongs to history and has become an exhibit in the obstetrical museum. Cardioflowgraphy shows high sensitivity, but low specificity in detection of fetal hypoxia. The pH determination represents an invasive method detecting only the current state of the fetus. As for the intrapartum fetal pulse oximetry, no decrease in the number of caesarean sections has been observed (increased number of operations performed). What about the ST analysis – is that finally the much sought-after method? The studies made on animals and people proved that intrapartum hypoxemia has an influence on the shape of the fetal ECG curve [22]. The future is seen in the diagnostic instruments combining the two methods of CTG and ST analysis in a single device. Computer-processed data remove any doubts regarding the evaluation of the recorded results. At present, the only diagnostic instruments available are the instruments applying internal monitoring with the help of the scalp electrode. In this study the authors present a system which may enable applying the gentler external monitoring in everyday medical practice.

### Adaptive filtration

As the principles of adaptive filtration are to be applied in this paper, this chapter is dedicated to progressive processing of numerical signals. Fig. 5 shows a basic block diagram of an adaptive filter [2].

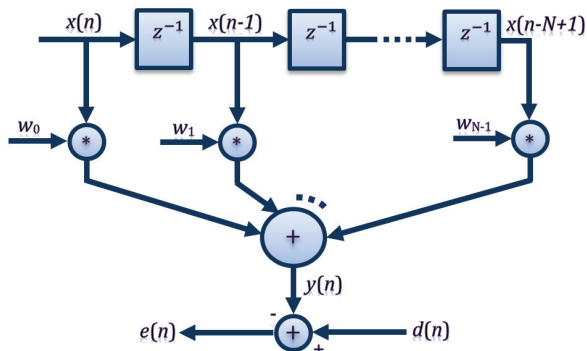


Fig.5. Block diagram of an adaptive filter

In Fig. 5,  $x(n)$  is the input sample vector,  $y(n)$  is the adaptive filter output,  $d(n)$  is the required response,  $e(n)$  is the error signal (estimated error),  $w_i$  represents the coefficients of the weight vector of the transversal FIR filter,  $z^{-1}$  is the delay.

In this paper, the input signal in the form of the column vector will be defined by equation:

$$(1) \mathbf{x}(n) = [x(n) \ x(n-1) \ x(n-2) \ \dots \ x(n-N+1)]^T$$

The weight vector of the transversal filter (which represents the coefficients of the adaptive FIR filter) will be expressed as follows:

$$(2) \mathbf{w}(n) = [w_0(n) \ w_1(n) \ w_2(n) \ \dots \ w_{N-1}(n)]^T$$

The output signal of the adaptive transversal filter may be expressed by the following equation:

$$(3) y(n) = \sum_{i=0}^{N-1} w_i(n)x(n-i)$$

It is an  $N$ -order filter, therefore the order range of 0 up to  $N-1$ . It can be seen that this is also equivalent to the dot product between the impulse response vector and the input vector, and alternatively the product of the transpose of the filter tap weight vector and the input vector, see equation 4. Both of these equalities will be used throughout the paper.

$$(4) \begin{aligned} y(n) &= \mathbf{w}(n) \cdot \mathbf{x}(n) \\ y(n) &= \mathbf{w}^T(n)\mathbf{x}(n) \end{aligned}$$

The aim of the whole process of weight adaptation is gradual reducing of the value of the cost function  $\zeta(n)$  [2] up to its minimum.  $\zeta(n)$  is only dependent on the values of the error function, i.e. it is dependent on the difference between the required and the actual value (that is the difference between the required and the actual output of the FIR filter):

$$(5) e(n) = d(n) - y(n)$$

The experiments performed included examination of the basic representatives of two classes of adaptive algorithms. The first class is usually referred to as the mean square error (MSE) [15] of the adaptive filter (LMS algorithm). The purpose of the whole process is gradual reducing of the cost function values  $\zeta(n)$  up to minimum (the minimum value of the mean square error) [3].

$$(6) \zeta(n) = E[e^2(n)] = E[(d(n) - y(n))^2]$$

The second class of adaptive algorithms is known as the recursive least square method (RLS) [15]. The basic difference from the LMS algorithms is the stochastic concept itself. The RLS method works with the mean values of variables calculated at time instants instead of the sample average means calculated from several realisations of a stochastic process [3].

$$(7) \begin{aligned} \zeta(n) &= \sum_{k=1}^n \rho_n(k) e_n^2(k) \\ \rho_n(k) &= \lambda^{n-k} \end{aligned}$$

where  $k = 1, 2, 3, \dots, n$ , parameter  $\lambda$  denotes the “forgetting factor” and is defined within the range of 0 to 1

### Wiener filter

Wiener filters [5] represent a special group of transversal FIR filters based on the MSE cost function given by equation 6, used to reach the optimum state of the weight vector of the transversal filter which reduces the MSE signal to minimum. These filters will be used to derive the adaptive filter algorithms hereinafter.

Let us consider the output from the transversal FIR filter, as stated in equation 3 or 4, for  $w(n)$  as the weight vector of the filter and  $x(n)$  as the input vector. The MSE cost function can be expressed in terms of the cross-correlation vector [5]

between the required and the input signals,  $\mathbf{p}(n) = E[\mathbf{x}(n) d(n)]$  and the auto-correlation matrix [5] of the input signal  $\mathbf{R}(n) = E[\mathbf{x}(n) \mathbf{x}^T(n)]$ .

$$\begin{aligned} \zeta &= E[e^2(n)] \\ &= E[(d(n) - y(n))^2] \\ (8) \quad &= E[d^2(n) - 2d(n)\mathbf{w}^T(n)\mathbf{x}(n) + \mathbf{w}^T(n)\mathbf{x}(n)\mathbf{x}^T(n)\mathbf{w}(n)] \\ &= E[d^2(n)] - 2E[\mathbf{w}^T(n)\mathbf{x}(n)] + E[\mathbf{w}^T(n)\mathbf{x}(n)\mathbf{x}^T(n)\mathbf{w}(n)] \\ &= E[d^2(n)] - 2\mathbf{w}^T\mathbf{p} + \mathbf{w}^T\mathbf{R}\mathbf{w} \end{aligned}$$

In case of its application in the FIR filtering, the above stated cost function becomes an  $N$ -dimensional square function. The minimum value of  $\zeta(n)$  can be found by means of equation in which the gradient of the filter weight is set to zero [2].

$$\begin{aligned} \frac{\partial}{\partial w_i} &= 0 \text{ for } i = 0, 1, \dots, N-1 \\ (9) \quad \nabla &= \left[ \frac{\partial}{\partial w_0} \quad \frac{\partial}{\partial w_1} \quad \dots \quad \frac{\partial}{\partial w_{N-1}} \right]^T \\ \nabla \zeta &= 0 \end{aligned}$$

By means of finding the equation gradient 8, setting it equal to zero and inverting the terms within the equation we obtain the optimum solution for the weight values of the Wiener filter  $\mathbf{w}_0$ :

$$\begin{aligned} \nabla \zeta &= 0 \\ (10) \quad 2\mathbf{R}\mathbf{w}_0 - 2\mathbf{p} &= 0 \\ \mathbf{w}_0 &= \mathbf{R}^{-1}\mathbf{p} \end{aligned}$$

The optimum Wiener solution consists in setting the filter weights in such a way that the cost function converges to zero. This vector may be found as a result of the inversion of the auto-correlation matrix of the input vector and the cross-correlation vector between the required signal and the input vector. The LMS algorithm of adaptive filtering tries to find the optimum Wiener solution using estimations based on the momentary values. For more details refer to [2], [3].

### LMS algorithm

With each iteration of the LMS algorithm, the tap weights of the adaptive filter are updated according to the following equation [5]:

$$(11) \quad \mathbf{w}(n+1) = \mathbf{w}(n) + 2\mu e(n)\mathbf{x}(n)$$

The  $\mu$  parameter denotes the step size. It is a small, positive constant which influences the properties of the algorithm adaptations (filter stability, convergence speed, etc.).

### Derivation of the LMS algorithm

The LMS algorithm is a basic representative of the class of stochastic gradient algorithms based on the Wiener filtration theory, stochastic average approximation and the

least mean square method. In fact, it is an approximation of the Wiener optimum filtration method, see Chapter Wiener filter. The algorithm iterates the tap weight of each signal in the filter in the direction of the gradient of the square amplitude of the error signal with regard to the signal tap weight in question; see the equation in [3]:

$$\begin{aligned} \mathbf{w}(n+1) &= \mathbf{w}(n) - \mu \nabla \zeta(n) \\ (12) \quad \text{where } \xi(n) &= E[e^2(n)] \end{aligned}$$

The LMS algorithm is an approximation of the steepest descent algorithm which utilises a momentary estimation of the gradient vector. It is a stochastic gradient adaptation in which the FIR filter is used [3]:

$$\begin{aligned} \mathbf{w}(n+1) &= \mathbf{w}(n) - \mu \nabla \xi(n) \\ (13) \quad \text{where } \xi(n) &= e^2(n) \end{aligned}$$

The gradient of the cost function  $\xi(n)$  may alternatively be expressed as:

$$\begin{aligned} \nabla \xi(n) &= \nabla (e^2(n)) \\ &= \frac{\partial e^2(n)}{\partial \mathbf{w}} \\ &= 2e(n) \frac{\partial e(n)}{\partial \mathbf{w}} \\ (14) \quad &= 2e(n) \frac{\partial (d(n) - y(n))}{\partial \mathbf{w}} \\ &= -2e(n) \frac{\partial \mathbf{e}\mathbf{w}^T(n)\mathbf{x}(n)}{\partial \mathbf{w}} \\ &= -2e(n)\mathbf{x}(n) \end{aligned}$$

If we put this resulting term back into equation 8, we obtain a relation for the LMS algorithm, given by equation 11.

### Implementation of the LMS algorithm

Each iteration of the LMS algorithm requires 3 different steps to be taken in the following order:

- The output from the FIR filter  $y(n)$  is computed by means of equation 3 or 4
- The estimated error value is computed by means of equation 5
- The tap weights of the FIR vector are updated in terms of preparation for the following iteration using equation 11

### RLS algorithm

RLS is a basic representative of the second class of adaptive algorithms – algorithms based on the Kalman filtration theory [5]. The basic difference from the LMS algorithm family is its own stochastic concept. The RLS method works with the mean values of variables calculated at time instants instead of the sample average means calculated from several realisations of a stochastic process [3]. The relation for the cost function is given by equation 7, which reveals the principle of time averaging. The filter structure remains the same as in the case of LMS algorithm, only the adaptive process is different with regard

to application of average means. As a result, RLS algorithms are characterised by much higher computational complexity than the LMS algorithms. This difference is so huge (RLS tasks are higher by one order than LMS tasks) that it often leads to conclusions that RLS algorithms have no practical usage. On the other hand, if we look at the convergence speed, we find out that the convergence speed of RLS is several times higher than that of LMS. This ensues from the application of time averaging, which predicts highly accurate values.

### Derivation of the RLS algorithm

The RLS cost function given by equation 7 indicates that within time  $n$  all the preceding estimated error values are required from the very moment of initiation of the RLS algorithm. To put it simply, as the time passes, the amount of data required for processing of the algorithm increases. Therefore, due to its limited memory and abilities, the RLS algorithm in its purest form is practically inapplicable. However, the derivation presumes processing of all the data. In practice, though, the processing only involves a finite number of preceding values corresponding to  $N$  sequence of the RLS FIR filter. To derive the algorithm, we first define  $y_n(k)$  as the FIR filter output,  $n$  as the currently used weight vector, and  $k$  as the input vector of the preceding time. The estimated error value  $e_n(k)$  is the difference between the required output within time  $k$ , and the corresponding value  $y_n(k)$ . These and other suitable definitions are expressed by means of equation 15, for  $k=1,2,3...n$  [3].

$$(15) \quad \begin{aligned} y_n(k) &= \mathbf{w}^T(n)\mathbf{x}(k) \\ e_n(k) &= d(k) - y_n(k) \\ \mathbf{d}(n) &= [d(1), d(2) \dots d(n)]^T \\ \mathbf{y}(n) &= [y_n(1), y_n(2) \dots y_n(n)]^T \\ \mathbf{e}(n) &= [e_n(1), e_n(2) \dots e_n(n)]^T \\ \mathbf{e}(n) &= \mathbf{d}(n) - \mathbf{y}(n) \end{aligned}$$

If we define  $\mathbf{X}(n)$  as the matrix consisting of  $n$  previous input column vector up to the present time, then  $\mathbf{y}(n)$  may alternatively be expressed as [3]:

$$(16) \quad \begin{aligned} \mathbf{X}(n) &= [\mathbf{x}(1), \mathbf{x}(2), \dots \mathbf{x}(n)] \\ \mathbf{y}(n) &= \mathbf{X}^T(n)\mathbf{w}(n) \end{aligned}$$

The cost function in equation 3 may be expressed in the form of a matrix vector using  $\mathbf{\Lambda}(n)$  of the diagonal matrix including the weighted coefficients.

$$(17) \quad \begin{aligned} \xi(n) &= \sum_{k=1}^n \lambda^{n-k} e_n^2(k) = \mathbf{e}^T(n) \tilde{\mathbf{\Lambda}}(n) \mathbf{e}(n) \\ \text{where } \tilde{\mathbf{\Lambda}}(n) &= \begin{bmatrix} \lambda^{n-1} & 0 & 0 & \dots & 0 \\ 0 & \lambda^{n-2} & 0 & \dots & 0 \\ 0 & 0 & \lambda^{n-3} & \dots & 0 \\ \dots & \dots & \dots & \dots & \dots \\ 0 & 0 & 0 & \dots & 1 \end{bmatrix} \end{aligned}$$

By putting in the values from equations 15 and 16, the cost functions may be extended and later reduced, as in equation 18.

$$(18) \quad \begin{aligned} \xi(n) &= \mathbf{e}^T(n) \tilde{\mathbf{\Lambda}}(n) \mathbf{e}(n) \\ &= \mathbf{d}^T \tilde{\mathbf{\Lambda}} \mathbf{d} - \mathbf{d}^T \tilde{\mathbf{\Lambda}} \mathbf{y} - \mathbf{y}^T \tilde{\mathbf{\Lambda}} \mathbf{d} + \mathbf{y}^T \tilde{\mathbf{\Lambda}} \mathbf{y} \\ &= \mathbf{d}^T \tilde{\mathbf{\Lambda}} \mathbf{d} - \mathbf{d}^T \tilde{\mathbf{\Lambda}} (\mathbf{X}^T \mathbf{w}) - (\mathbf{X}^T \mathbf{w})^T \tilde{\mathbf{\Lambda}} \mathbf{d} + (\mathbf{X}^T \mathbf{w})^T \tilde{\mathbf{\Lambda}} (\mathbf{X}^T \mathbf{w}) \\ &= \mathbf{d}^T \tilde{\mathbf{\Lambda}} \mathbf{d} - 2 \tilde{\boldsymbol{\theta}}_\lambda^T \mathbf{w} + \mathbf{w}^T \tilde{\boldsymbol{\Psi}}_\lambda \mathbf{w} \end{aligned}$$

where  $\tilde{\boldsymbol{\Psi}}_\lambda \mathbf{w}(n) = \mathbf{X}(n) \tilde{\mathbf{\Lambda}}(n) \mathbf{X}^T(n)$   
 $\tilde{\boldsymbol{\theta}}_\lambda(n) = \mathbf{X}(n) \tilde{\mathbf{\Lambda}}(n) \mathbf{d}(n)$

Then we derive the gradient of the above stated cost function formula with regard to the filter weights. By means of making it converge to zero, we obtain the coefficients of the  $\tilde{\mathbf{w}}(n)$  filter which minimises the cost function.

$$(19) \quad \begin{aligned} \tilde{\boldsymbol{\Psi}}_\lambda(n) \tilde{\mathbf{w}}(n) &= \tilde{\boldsymbol{\theta}}_\lambda(n) \\ \tilde{\mathbf{w}}(n) &= \tilde{\boldsymbol{\Psi}}_\lambda^{-1}(n) \tilde{\boldsymbol{\theta}}_\lambda(n) \end{aligned}$$

In this way the  $\boldsymbol{\Psi}(n)$  matrix may be extended and later rearranged in the recursive layout, which may then be used for a special form of lemma inverse matrix in order to find the inverse matrix required for the computation of the weight vector update. The  $\mathbf{k}(n)$  vector, known as the amplifying vector, is included in order to simplify the computation [3].

$$(20) \quad \begin{aligned} \tilde{\boldsymbol{\Psi}}_\lambda^{-1}(n) &= \lambda \tilde{\boldsymbol{\Psi}}_\lambda^{-1}(n-1) + \mathbf{x}(n) \mathbf{x}^T(n) \\ &= \lambda^{-1} \tilde{\boldsymbol{\Psi}}_\lambda^{-1}(n-1) - \frac{\lambda^{-2} \tilde{\boldsymbol{\Psi}}_\lambda^{-1}(n-1) \mathbf{x}(n) \mathbf{x}^T(n) \tilde{\boldsymbol{\Psi}}_\lambda^{-1}(n-1)}{1 + \lambda^{-1} \mathbf{x}^T(n) \tilde{\boldsymbol{\Psi}}_\lambda^{-1}(n-1) \mathbf{x}(n)} \\ &= \lambda^{-1} (\tilde{\boldsymbol{\Psi}}_\lambda^{-1}(n-1) - \mathbf{k}(n) \mathbf{x}^T(n) \tilde{\boldsymbol{\Psi}}_\lambda^{-1}(n-1)) \end{aligned}$$

where  $\mathbf{k}(n) = \frac{\lambda^{-1} \tilde{\boldsymbol{\Psi}}_\lambda^{-1}(n-1) \mathbf{x}(n)}{1 + \lambda^{-1} \mathbf{x}^T(n) \tilde{\boldsymbol{\Psi}}_\lambda^{-1}(n-1) \mathbf{x}(n)}$   
 $= \tilde{\boldsymbol{\Psi}}_\lambda^{-1}(n) \mathbf{x}(n)$

The  $\tilde{\boldsymbol{\theta}}_\lambda(n)$  vector given by equation 18 may also be expressed in the recursive form. By substituting this expression for  $\boldsymbol{\Psi}^{-1}$  from equation 20 into equation 19, we may finally get the weight filter vector for the RLS algorithm, as in equation 21.

$$(21) \quad \begin{aligned} \tilde{\boldsymbol{\theta}}_\lambda(n) &= \lambda \tilde{\boldsymbol{\theta}}_\lambda(n-1) + \mathbf{x}(n) \mathbf{d}(n) \\ \tilde{\mathbf{w}}(n) &= \tilde{\boldsymbol{\Psi}}_\lambda^{-1}(n) \tilde{\boldsymbol{\theta}}_\lambda(n) \\ &= \tilde{\boldsymbol{\Psi}}_\lambda^{-1}(n-1) \tilde{\boldsymbol{\theta}}_\lambda(n-1) - \mathbf{k}(n) \mathbf{x}^T(n) \tilde{\boldsymbol{\Psi}}_\lambda^{-1}(n-1) \tilde{\boldsymbol{\theta}}_\lambda(n-1) + \mathbf{k}(n) \mathbf{d}(n) \\ &= \tilde{\mathbf{w}}(n-1) - \mathbf{k}(n) \mathbf{x}^T(n) \tilde{\mathbf{w}}(n-1) + \mathbf{k}(n) \mathbf{d}(n) \\ &= \tilde{\mathbf{w}}(n-1) + \mathbf{k}(n) (\mathbf{d}(n) - \tilde{\mathbf{w}}^T(n-1) \mathbf{x}(n)) \\ \tilde{\mathbf{w}}(n) &= \tilde{\mathbf{w}}(n-1) + \mathbf{k}(n) \bar{e}_{n-1}(n) \end{aligned}$$

where  $\bar{e}_{n-1}(n) = \mathbf{d}(n) - \tilde{\mathbf{w}}^T(n-1) \mathbf{x}(n)$

### Implementation of the RLS algorithm

As mentioned earlier in this paper, the memory of the RLS algorithm is limited by the finite number of values corresponding to the sequence of the filter weight vector. In this context, two aspects of the RLS implementation have to be mentioned: First, while the inverse matrix is essential for derivation of the RLS algorithm, the computation of the inverse matrix is not needed for the implementation itself, which considerably reduces the computational complexity of the algorithm. Second, contrary to the algorithms based on LMS, the current variables are updated in terms of iterations and used together with the values of the preceding iteration.

To implement the RLS algorithm, the following steps must be performed in the order stated below:

The filter output is calculated using the filter weights from the preceding iteration and the current input vector:

$$(22) \quad \bar{y}_{n-1}(n) = \bar{\mathbf{w}}^T(n-1)\mathbf{x}(n)$$

The medium amplification vector is calculated by means of equation:

$$(23) \quad \mathbf{u}(n) = \tilde{\Psi}_\lambda^{-1}(n-1)\mathbf{x}(n)$$

$$\mathbf{k}(n) = \frac{1}{\lambda + \mathbf{x}^T(n)\mathbf{u}(n)}\mathbf{u}(n)$$

The estimated error value is calculated by means of equation:

$$(24) \quad \bar{e}_{n-1}(n) = d(n) - \bar{y}_{n-1}(n)$$

The filter weight vector is updated using equation 24 and the amplification vector is given by equation 23:

$$(25) \quad \mathbf{w}(n) = \bar{\mathbf{w}}^T(n-1) + \mathbf{k}(n)\bar{e}_{n-1}(n)$$

The inverse matrix is computed by means of equation:

$$(26) \quad \tilde{\Psi}_\lambda^{-1}(n) = \lambda^{-1}(\tilde{\Psi}_\lambda^{-1}(n-1) - \mathbf{k}(n)\mathbf{x}^T(n)\tilde{\Psi}_\lambda^{-1}(n-1))$$

### The designed adaptive system

Fig. 6 shows a principal diagram of the designed adaptive system within which the simulations were performed. The concept of this diagram was implemented in the Matlab environment [4] using the source code for commands (no source libraries for adaptive filtration were used as our aim was to reach better debugging of the program).

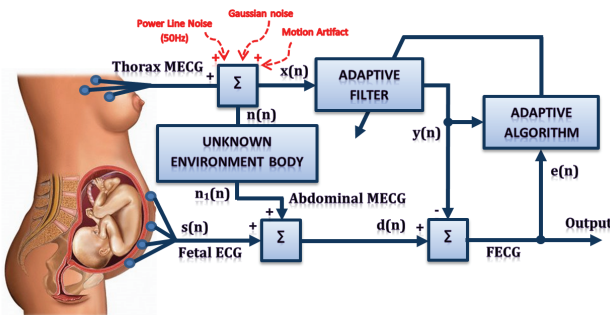


Fig.6. The designed adaptive system

The designed adaptive system includes two input channels. The first (primary) channel represents the FECG (with the amplitude range of 10 - 300  $\mu\text{V}$ ) detected by the electrodes placed on the mother's abdomen (here the required FECG is distorted by the much stronger MECG (Fig. 3) and a number of other undesirable disturbances (Fig. 6). The second (reference) channel represents the MECG (with the amplitude range of 50  $\mu\text{V}$  - 5 mV) detected by the electrodes placed on the mother's thorax.

Thus we basically have to deal with two hearts (signal sources: heart of the fetus – useful signal, mother's heart – disturbing signal) which are electrically isolated and work independently.

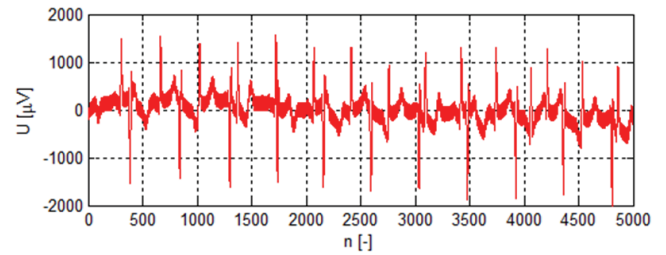


Fig.7. The FECG distorted by the stronger signal and modelled noises

The simplest way of suppressing the undesired MECG in the FECG seems to be a direct subtraction of the MECG from the FECG. However, this technique does not work as the MECG recorded at the primary input is not quite the same as the MECG at the reference input. This is due to the unknown human body environment (signal deformation due to the surrounding environment – delay, interference, etc.). The MECG is further distorted by a series of other disturbances all of which were taken into consideration in our experiments.

It is shown in Fig. 6 that the reference channel only records the MECG  $n(n)$ . The primary microphone records the FECG  $s(n)$  and the MECG after passing through the unknown environment  $n_1(n)$ . The auxiliary signal is then given by the following relation:

$$(27) \quad d(n) = s(n) + n_1(n)$$

Further, various noises were taken into consideration within the performed simulation (power line interference, motion artifacts, Gaussian noise). These noises were modelled onto the reference channel. The fact that the MECG of the reference channel is not identical with the MECG of the primary channel (due to the unknown human body environment) was simulated as the FIR  $N$ -order filter ( $N=13$  was selected for representation, see Fig. 9). If we model the way from the MECG source to the primary channel as a linear system, we can formulate such an adaptive algorithm that will teach the FIR filter to distinguish the channel characteristics. If this filter is later used for the noise detected by the reference microphone, we are able to successfully subtract the noise detected by the primary channel. The aim of the designed system is therefore to suppress the undesired MECG including other noises, such as 50Hz power line interference, Gaussian noise and motion artifacts, in the FECG (Fig. 8).

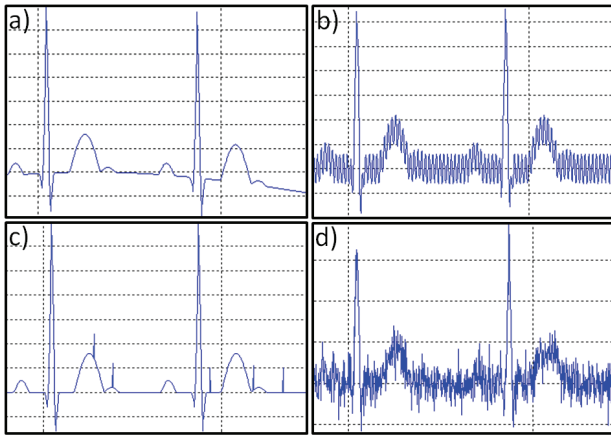


Fig.8. The interference applied: a) motion artifacts, b) power line interference 50Hz, c) impulse interference, d) Gaussian noise

### Results of the performed experiments

Fig. 9 shows the filter frequency characteristics for simulation of the unknown human body environment (the characteristics is based on real measurements). It represents the ideal wave form as well as the wave forms learnt by the examined algorithms (the filter order was  $N=13$ , the measurements for various values of  $N$  are summarised in Table 1).

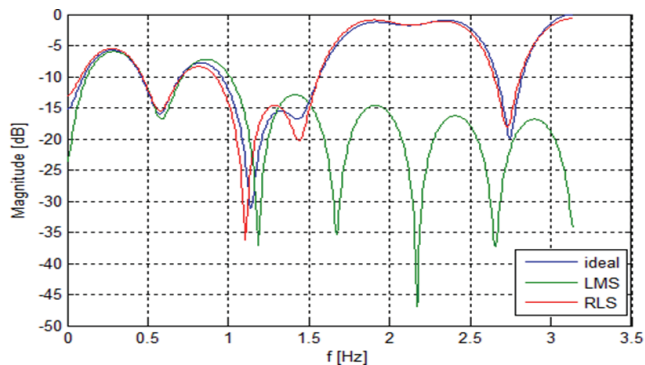


Fig.9. The frequency characteristic of the simulated unknown human body environment for  $N=13$  (ability of LMS, RLS to learn the frequency characteristic)

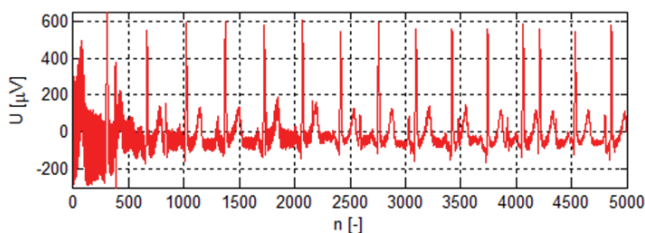


Fig.10. The output after filtration using the LMS algorithm

For the simulations, the first  $n=5000$  samples of the real ECG signal recordings were used. The LMS adaptive algorithm was tested in the first place. Zero was selected for the first set of the adaptation process coefficients (by means of generating a zero matrix). In the case of LMS algorithm, it is important to set the value of the step size (convergence constant). The value of the convergence constant  $\mu$ , which was determined experimentally, has a critical importance for the convergence speed and stability of LMS algorithm. For  $\mu = 2.5e-9$  the stability was reached in 8s, for  $\mu = 3e-9$  in 6s, for  $\mu = 5e-9$  in 4s, for  $\mu = 1e-8$  in 2s. While searching for the optimum value, we observed the rule that the algorithm should converge at high speed and keep stable. The performed experiments revealed that a

higher convergence speed is reached at the expense of stability. Therefore we set  $\mu = 3e-9$ . Fig. 10 shows the output using the LMS algorithm.

The second algorithm under examination was the RLS algorithm. In this case we set the value of the forgetting coefficient  $\lambda = 0,98$ . Fig. 11 shows the output reached by means of RLS algorithm.

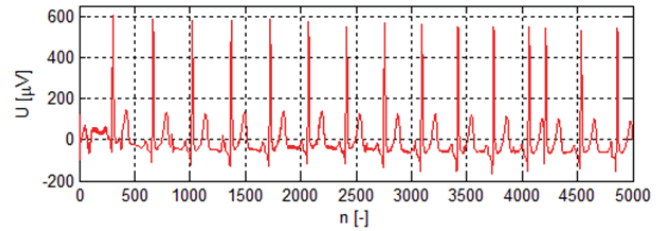


Fig.11. The output after filtration using the RLS algorithm

Figures 12-13 show the MSE (mean square error) of the both algorithms in question.

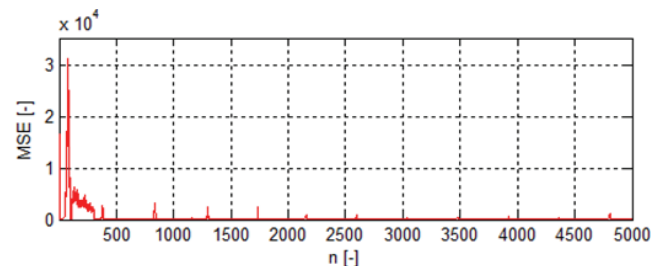


Fig.12. The square error learning curve of RLS algorithm

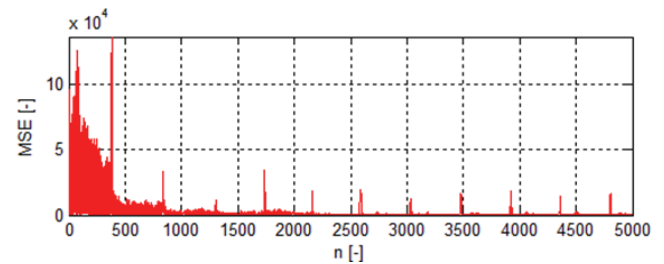


Fig.13. The square error learning curve of LMS algorithm

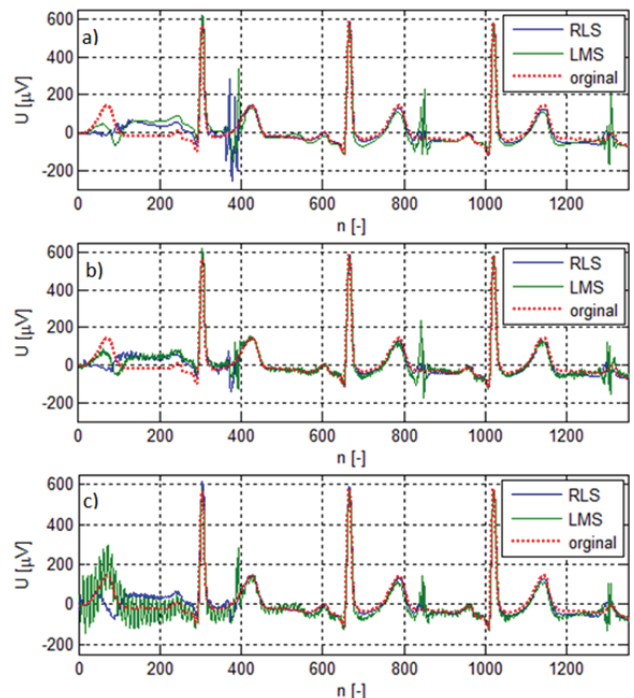


Fig.14. A detail of the FECG output signal for several variants

Figures 14 a), b), c) represent the output details obtained with the help of the adaptive system. They show individual results for several variants at the filter output: a) FECCG + MECG + motion artifacts b) FECCG + MMECG + motion artifacts + power line interference 50 Hz c) FECCG + MMECG + motion artifacts + power line interference + Gaussian noise.

Fig. 15 represents the individual signal spectra of the performed simulation.

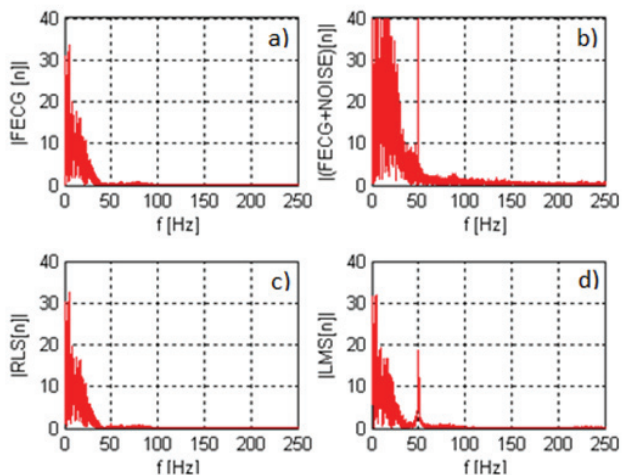


Fig.15. The individual signal spectra during the analysis: a) clean FECCG, b) noised FECCG, c) RLS output, d) LMS output

Fig. 16 shows the individual signal details in terms of the ST segment analysis. Fig. 16 a) represents the output using the LMS algorithm and Fig. 16 b) shows the output using the RLS algorithm. If we look back at Fig. 7, representing the distorted FECCG signal, it is obvious that we are only able to analyse the R-R interval, i.e. the time segment between the individual heart beats of the fetus. It is impossible to make analysis using the complete ECG. If we look at Fig. 16, we can state that the designed adaptive system is able to detect the complete fetal ECG curve. On the ECG curve, the amplitude of the QRS complex, the denivelation of the ST segment against the isoelectric baseline and the T wave height are monitored. It is therefore possible to use the principles of the STAN analysis. The average ECG wave is determined several times per minute and from that the ratio between the QRS complex and the T wave amplitude, the so called T/QRS ratio, is derived. For more details refer to [22].

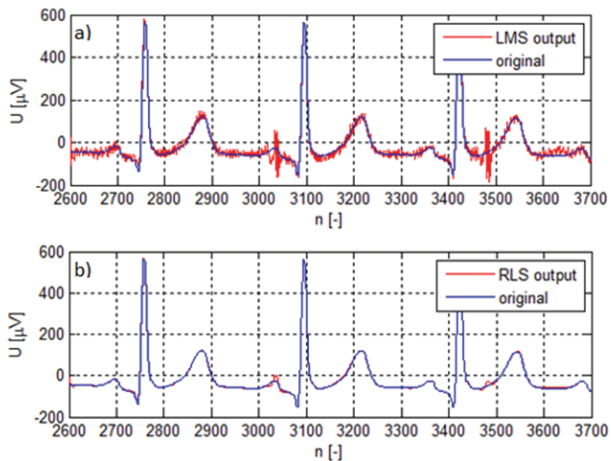


Fig.16. The individual signal details in terms of the ST segment analysis

Fig. 17 shows the coefficient behaviour during filtration for the both algorithms under examination. For the sake of better transparency, the graph only indicates behaviour of a single coefficient.

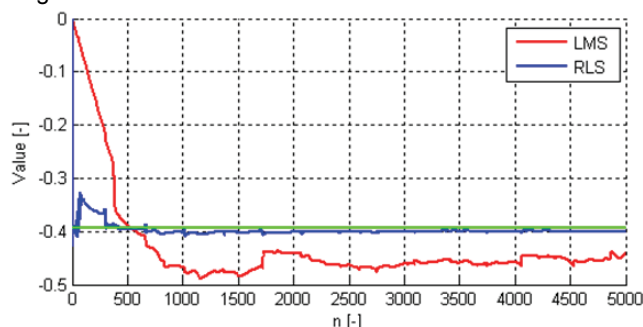


Fig.17. The coefficient behaviour during filtration

Figures 18 - 21 represent the spectrograms of the individual signals.

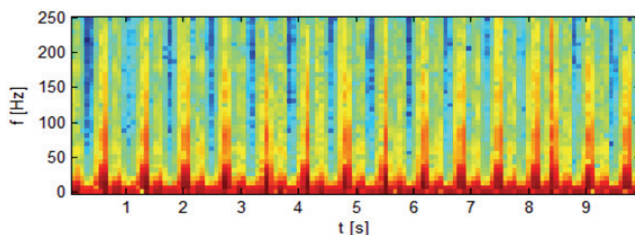


Fig.18. FECCG  $s(n)$  – primary signal

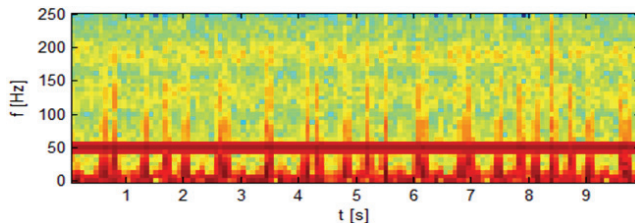


Fig.19. Auxiliary signal  $d(n)$  – combination of FECCG + MECG + noises

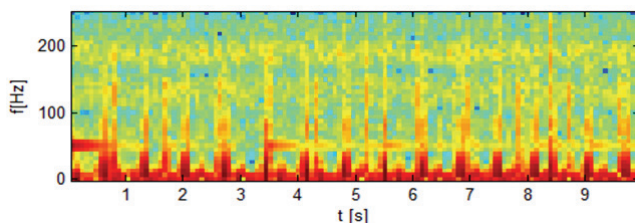


Fig.20. The output using the LMS algorithm

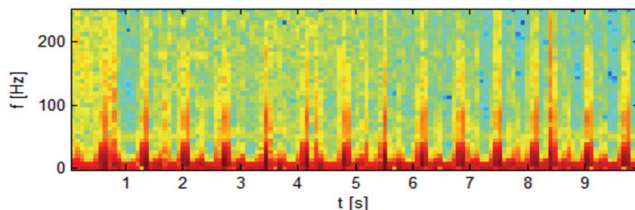


Fig.21. The output using the RLS algorithm

Table 1 shows the ability of the adaptive algorithms to improve the SNR value (signal-to-noise ratio) in relation to the filter length. The performed experiments included the determination of the SNR value of the noised FECCG (primary channel) and subsequently the determination of the value of the signal after passing through the adaptive system (the output after filtration). The difference between the two values revealed what level of improvement had been reached by the both algorithms in question. The SNR

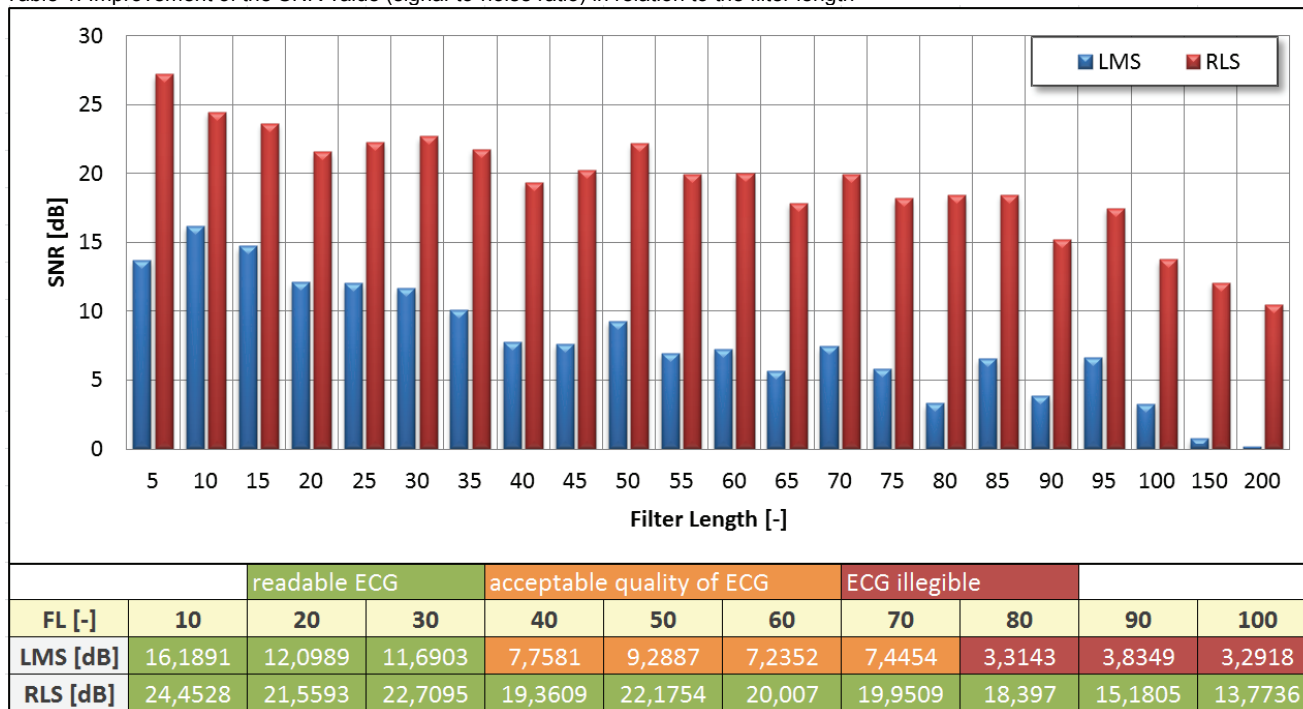
is defined by the following relation [16]:

$$(28) \quad SNR = 10 \log \frac{P_s}{P_n} [dB],$$

where the  $P_s$  and  $P_n$  variables denote the performance of

the signal ( $s$  refers to signals) and the noise ( $n$  refers to noise). If  $SNR = 0$  dB, it means that both the signal and the noise give the same performance. If  $SNR > 0$ , the performance of the useful signal is higher than that of the noise; if  $SNR < 0$ , it is vice versa.

Table 1. Improvement of the SNR value (signal-to-noise ratio) in relation to the filter length



### Conclusion

The experiments made on the real ECG signals revealed that the designed system adaptive system may considerably improve the informative value of the fetal ECG in terms of external monitoring. The improvement is so great that it enables a clinical diagnostics of the ST segment of the ECG curve, which was otherwise only possible in case of the invasive internal monitoring.

The experiments revealed that the LMS and RLS algorithms subjected to examination have desirable properties for applications designed to eliminate all sorts of interference from the FECG signals. It has been proved that the RLS algorithm has better filtration properties irrespective of the character of the signal or the noise (Fig. 14). The RLS algorithm appears to be particularly convenient for use if the signal is characterised by sudden changes of amplitude or frequency. RLS needs a longer time for computation, especially for longer filter lengths. The change in the filter length has little impact on the convergence behaviour of the RLS algorithm (Table 1). In the case of the LMS algorithm, an increase in the filter length means a considerable impairment of its convergence behaviour (Table 1). The LMS adaptive algorithm under examination is simple and mathematically undemanding. However, in tests it reached a lower convergence speed and a higher error rate of the filtration process (Fig. 12). On the contrary, the RLS algorithm is mathematically highly complex. Nevertheless, the test results have shown that it is very precise. It shows a low error rate and extremely high convergence speed (Fig. 11). Therefore it seems that for the designed system the aim of which is to improve the monitoring quality of the fetal electrocardiogram as a

modern tool in prediction of the intrapartum fetal hypoxia, the application of the RLS algorithm is a better alternative, on condition that the system is not limited by the higher computational complexity of this algorithm.

The experimental results have proved that the adaptive system with the implemented RLS algorithm can be used with the external STAN system which is utilised for prediction of the intrapartum fetal hypoxia. The results using the RLS algorithm meet the high demands for the quality of the FECG curve. Signal procession by means of the adaptive system removes any doubts about the evaluation of the results (diagnostics). The authors of this paper have presented a concept of the adaptive system which could be used in medical practice for gentler external monitoring without losing the advantages of internal monitoring.

### REFERENCES

- [1] MARTINEK, Radek; ZIDEK, Jan. Use of adaptive filtering for noise reduction in communications systems. *International Conference-Applied Electronics*. Pilsen: AE, 2010. pp. 1-6, ISBN 978-80-7043-865-7, ISSN 1803-7232, INSPEC Accession Number 11579482.
- [2] DINIZ, Poulou S. R. *Adaptive Filtering: Algorithms and Practical Implementation*. 3rd ed., New York : Springer, 2008. 632 p., ISBN 978-0-387-31274-3.
- [3] FARHANG-BOROJENY, B. *Adaptive Filters: Theory and Applications*. New York : John Wiley and Sons, 1999. 548 p., ISBN 978-0471983378.
- [4] POULARIKAS, Alexander D.; RAMADAN, Zayed M. *Adaptive Filtering Primer with MATLAB*. New York, USA : CRC Press, 2006. 202 s. ISBN 978-0-8493-7043-4.
- [5] HAYKIN, Simon. *Adaptive Filter Theor.* 4th. New Jersey : Prentice Hall, 2001. 920 p. ISBN 978-0130901262.

- [6] SVATOŠ, Josef. *Biologické signály I: Geneze, zpracování a analýza*. 2. Praha: ČVUT, 1998. 202 p. ISBN 80-01-01822-9.
- [7] CABANISS, Micki L.; ROSS, Michael G. *Fetal Monitoring Interpretation*. Second.: Lippincott Williams & Wilkins, 2009. 512 p. ISBN 978-1-60831-381-5.
- [8] ROSÉ, K.G.; LUZIETT, R. The fetal electrocardiogram : ST waveform analysis during labour. *Journal of Perinatal Medicine*. 1994, 22, pp. 502-512.
- [9] KHAMENE, A.; NEGAHDARIPOUR, S. A new method for the extraction of fetal ECG from the composite abdominal signal. *IEEE Trans. on Biomed. Eng.*. April 2000, vol. 47, n.4, pp. 507-515.
- [10] ROBERTS, M.J. *Signals and Systems : Analysis Using Transform Methods and MATLAB*. USA : The McGraw-Hill Companies, 2008. 1026 p. ISBN 0-07-293044-6.
- [11] HAMPTON, John R. *EKG stručně, jasně, přehledně*. 6<sup>th</sup> edition, Grada, 2005. 152 p. ISBN 80-247-0960-0.
- [12] Amer-Wahlin, I., Yli, B., Arulkumaran, S.: Fetal ECG and STAN technology—a review. *Eur Clinics Obstet Gynaecol* 2005, 1, 61–73.
- [13] WAGNER, Galen S. *Marriott's Practical Electrocardiography*. 8th edition Lippincott Williams & Wilkins, 2002. 488 p. ISBN 0781797381.
- [14] SORNMO, Leif; LAGUNA, Pablo. *Bioelectrical Signal Processing in Cardiac and Neurological Applications (Biomedical Engineering)*. 1st edition Academic Press, 2005. 688 p. ISBN 0124375529.
- [15] JAN, Jiří. *Číslíková filtrace, analýza a rekonstrukce signálů*. 2<sup>nd</sup> revised edition. Brno : VUTUM, 2002. 428 s. ISBN 80-214-1558-4.
- [16] BLANCHET, Gérard, CHARBIT, Maurice. *Digital Signal and Image Processing using MATLAB®*. Newport Beach, CA 92663, USA : ISTE USA, 2006. 764 p. ISBN 978-1-905209-13-2.
- [17] ZAPLATÍLEK, Karel, DOŇAR, Bohuslav. *MATLAB : začínáme se signály*. 1<sup>st</sup> edition. Praha : BEN – technical literature, 2006. 271 p. ISBN 80-7300-200-0.
- [18] ZAPLATÍLEK, Karel, DOŇAR, Bohuslav. *MATLAB : tvorba uživatelských aplikací*. 1<sup>st</sup> edition. Praha : BEN – technical literature, 2004. 215 p. ISBN 80-7300-133-0.
- [19] HUTSON, Michael. *Acoustic Echo using Digital Signal Processing*. Queensland, Australia, 2003. 78 p. The University of Queensland. Diploma thesis supervisor: Professor Simon Kaplan.
- [20] KARBAN, Pavel. *Výpočty a simulace v programech Matlab a Simulink*. 1<sup>st</sup> edition. Brno : Computer Press, a.s., 2006. 220 p. ISBN 80-251-1301-9.
- [21] HRUBAN, L.; JANKŮ, P. Analýza ST úseku EKG křivky plodu v průběhu porodu. *Praktický gynekolog*. 2005. WWW: <[http://www.praktickagynekologie.cz/pdf/pg\\_05\\_04\\_03.pdf](http://www.praktickagynekologie.cz/pdf/pg_05_04_03.pdf)>, ISSN 1801-8750.
- [22] JANKŮ, Petr. Analýza ST úseku fetálního EKG v intrapartální diagnostice hypoxie plodu u rizikových gravidit. Praha, 2007. 78 p. Diploma thesis. Masaryk University, Faculty of Medicine, WWW: <[http://is.muni.cz/th/38558/lf\\_d/Disertacni\\_prace\\_Janku1\\_2\\_.pdf](http://is.muni.cz/th/38558/lf_d/Disertacni_prace_Janku1_2_.pdf)>.
- [23] L. D. Lathauwer, B. D. Moor and J. Vandewalle, "Fetal electrocardiogram extraction by blind source subspace separation", *IEEE Trans. on Biomed. Eng.*, vol. 47 (5), pp. 567-572, May 2000
- [24] LATHAUWE, Lieven De; MOOR, Bart De; VANDEWALLE, Joos. Fetal Electrocardiogram Extraction by Blind Source Subspace Separation. *IEEE TRANSACTIONS ON BIOMEDICAL ENGINEERING*, May 2000, WWW: <<http://perso-etis.ensea.fr/~lathauwer/ldl-99-98.pdf>>, pp. 567-572 ISSN 0018-9299.
- [25] GAO, Ping; CHIEN CHANG, Ee; WYSE, Lonca. BLIND SEPARATION OF FETAL ECG FROM SINGLE MIXTURE USING SVD AND ICA. *ICICS-PCM*. Singapore, December 2003. WWW: <[http://www.zwhome.org/~lonca/Publications/Publications\\_files/GaoChienWyse03.pdf](http://www.zwhome.org/~lonca/Publications/Publications_files/GaoChienWyse03.pdf)>. ISSN 0-7803-8185-8.
- [26] ZARZOSO, Vicente; NANDI, Asoke K. Noninvasive Fetal Electrocardiogram Extraction: Blind Separation Versus Adaptive Noise Cancellation. *IEEE TRANSACTIONS ON BIOMEDICAL ENGINEERING*. JANUARY 2001. WWW: <<http://www.i3s.unice.fr/~zarzoso/biblio/tbme01.pdf>>. ISSN 0018-9294.
- [27] JAFARIM, G. ; CHAMBERS J. A. , Fetal electrocardiogram extraction by sequential source separation in the wavelet domain, *IEEE Trans. on Biomed. Eng.*, vol. 52 (3), pp. 390-400, March 2005. ISSN: 0018-9294.
- [28] JAFARI ,M.G. ; CHAMBERS ,J.A., Adaptive noise cancellation and blind source separation, *Proc. of the 4th Intl. Symp. Independent Component Analysis and Blind Signal Separation*, Nara, Japan, April 2003, pp. 627-632.
- [29] BARROS, A. K. ; OHNISHI, N., Fetal heart rate variability extraction by frequency tracking , *Proc. of the 3rd Intl. Conf. Independent Component Analysis and Source Separation*, San Diego, CA, USA, 2001.
- [30] ZENG, Yanjun ; LIU, Shijin ; ZHANG, Jianhua. Extraction of Fetal ECG Signal via Adaptive Noise Cancellation Approach. *Bioinformatics and Biomedical Engineering, ICBBE*, 2008. The 2nd International Conference. www ISBN 978-1-4244-1747-6.

---

**Authors:** Ing. Radek Martinek, E-mail: [radek.martinek.st1@vsb.cz](mailto:radek.martinek.st1@vsb.cz)  
 doc. Ing. Jan Zidek, CSc. E-mail: [jan.zidek@vsb.cz](mailto:jan.zidek@vsb.cz)  
 VSB-TU, Faculty of Electrical Engineering and Computer Science.  
 17. listopadu 15, 708 33 Ostrava-Poruba